On-line Model Structure Selection for Estimation of Plasma Boundary in a Tokamak

Journal of Physics: Conference Series **659** (2015) 012010 doi:10.1088/1742-6596/659/1/012010

On-line Model Structure Selection for Estimation of Plasma Boundary in a Tokamak

Vít Škvára[1], **Václav Šmídl**[1], **Jakub Urban**[2]

[1]Institute of Information Theory and Automation, Prague, Czech Republic,
[2]Institute of Plasma Physics, Prague, Czech Republic,

Abstract. Control of the plasma field in the tokamak requires reliable estimation of the plasma boundary. The plasma boundary is given by a complex mathematical model and the only available measurements are responses of induction coils around the plasma. For the purpose of boundary estimation the model can be reduced to simple linear regression with potentially infinitely many elements. The number of elements must be selected manually and this choice significantly influences the resulting shape. In this paper, we investigate the use of formal model structure estimation techniques for the problem. Specifically, we formulate a sparse least squares estimator using the automatic relevance principle. The resulting algorithm is a repetitive evaluation of the least squares problem which could be computed in real time. Performance of the resulting algorithm is illustrated on simulated data and evaluated with respect to a more detailed and computationally costly model FREEBIE.

1. Introduction

Tokamak is one the most promising concepts for future thermonuclear fusion reactors. In a tokamak, hot plasma is confined by a combination of strong toroidal and poloidal magnetic fields. The almost negligible weight of the plasma dictates that magnetohydrodynamic (MHD) equilibrium, i.e. a force-free state, describes its macroscopic evolution. MHD decsription includes also the plasma boundary (the so-called last closed flux surface), which must be controlled during a tokamak discharge because of performance and safety reasons. Real-time feedback control is necessary since the plasma behaviour cannot be reliably predicted, particularly because the equilibrium is unstable. Such a feedback control requires the plasma boundary as an input in real-time. See e.g. [1] or [2] for more details.

One of the possibilities for real-time plasma shape reconstruction is offered by magnetic sensors near the plasma boundary. However, full reconstruction of the equilibrium magnetic field (which includes the plasma shape) is a complex task due to non-linear behavior of the plasma. In [3], it was shown that the plasma boundary can be modeled by a linear combination of its base functions. Since the base functions are known, the estimation problem can be formulated as a simple linear regression with unknown number of regressors. Our task is to select the relevant subset of base functions of the model.

Selection of the structure of the linear model is a well studied problem in statistics and strong point of the Bayesian hypothesis testing. The conventional least squares problem is equivalent to maximum likelihood estimation of the linear Gaussian model. Selection of structure of this model is a conventional problem requiring to formalize two steps: i) to choose prior distribution of the

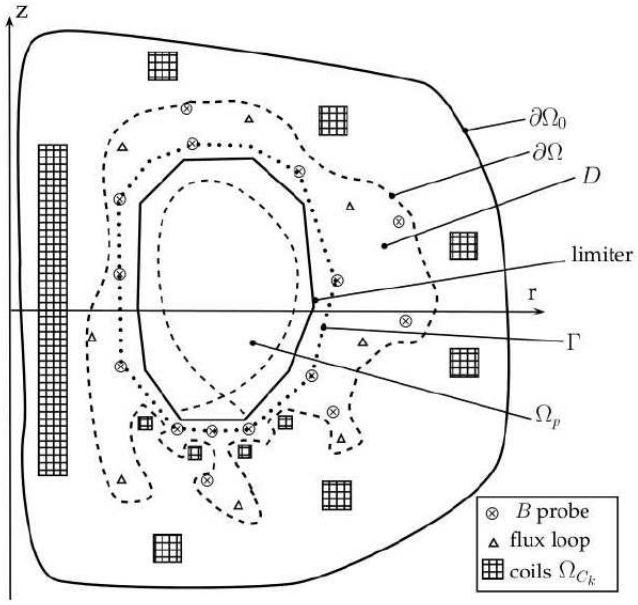

Figure 1. Tokamak section schema with measuring and shaping coils. *B probe* measures local magnetic field size, *flux loop* is a coil measuring magnetic flux ψ and Ω_{C_k} is a plasma shaping coil. Different contours important for plasma boundary reconstruction are denoted. *Limiter* is the inner surface of tokamak chamber, Ω_p is the plasma itself, delimited by dashed line. In the bottom of plasma we can observe an x-point, which is crucial for ensuring plasma stability. From [3].

parameters, and ii) to evaluate likelihoods corresponding to structures consisting of all significant combinations of regressors whose supply grows exponentially with the number of candidates.

A range of techniques arise by combination of different options for each step. This step is very important since the choice of a non-informative prior is inappropriate as it yields posterior Bayes factors dependent on an arbitrary multiplicative constant [4]. Many possibilities, including ridge regression, mixture priors, or g priors were tried, see review in [5] . Once the prior is chosen, many algorithms searching the space of solution are available using e.g. stochastic search [6], dynamic programming [7], MCMC approach [8] or variational approaches [9, 10].

In this paper, we are interested in estimation of the structure in real time for the purpose of tokamak control. Therefore, we seek an approach with simple implementation. One such possibility is the automatic relevance determination principle [11] which uses a hierarchical prior to suppress the regressors that are redundant. This technique uses the Variational Bayes approximation [12] which can be easily extended to dynamical systems [13].

The paper is organized as follows. In the second Section we introduce model of the plasma boundary is introduced in the form of linear regression. A model of Bayesian regularization of the linear regression model is introduced in the third Section and its Variational Bayes solution is presented. Experimental validation of the approach on simulated data from a real tokamak are presented in the fourth Section.

2. Model of plasma Boundary

Feedback control of plasma in a tokamak requires on-line reconstruction of the plasma boundary. The quality of the reconstruction is highly significant for tokamak operation safety and

performance. Two different kinds of measurements, which are typically available on a tokamak, are considered here to determine the shape: magnetic coils measuring local magnetic field B and flux loops measuring the poloidal magnetic flux ψ.

Following [3], we will formulate the model in the standard cylindric coordinates (r, ϕ, z) that are used in tokamak geometry description. Using the assumption of symmetry of plasma in toroidal direction of plasma chamber, we omit ϕ. Then, we carry out a transformation from (r, z) to toroidal coordinates $(\zeta, \eta) \in \mathbb{R}^+ \times \langle 0, 2\pi)$ around a pole $F_0 = (r_0, z_0)$, given by [14]

$$r = \frac{r_0 \sinh \zeta}{\cosh \zeta - \cos \eta}, \tag{1}$$

$$z = z_0 + \frac{r_0 \sin \eta}{\cosh \zeta - \cos \eta}. \tag{2}$$

Now let us assume that we have three sets of measurements available:

(i) N_f measurements of magnetic flux in coordinates $x_i^f = (r_i^f, z_i^f)$, $\psi_i^{meas} \approx \psi(x_i^f)$,
(ii) N_s measurements of magnetic flux gradient between two points x_i^1, x_i^2, $\delta_i \psi^{meas} = \psi(x_i^1) - \psi(x_i^2)$,
(iii) N_B measurements of magnetic field in points x_i^B and directions d_i, $B_i^{meas} \approx B(x_i^B) d_i$.

Next, we utilize the following decomposition of the flux estimate $\hat{\psi}(\zeta, \eta)$ into a system of toroidal harmonics

$$\hat{\psi} = \hat{\psi}_{ext} + \hat{\psi}_{int}, \tag{3}$$

$$\begin{aligned} \hat{\psi}_{ext}(\zeta, \eta) = & \frac{r_0 \sinh \zeta}{\sqrt{\cosh \zeta - \cos \eta}} \times \\ & \left\{ \sum_{n=0}^{M_{ea}} a_n^e Q_{n-1/2}^1(\cosh \zeta) \cos(n\eta) + \sum_{n=1}^{M_{eb}} b_n^e Q_{n-1/2}^1(\cosh \zeta) \sin(n\eta) \right\}, \end{aligned} \tag{4}$$

$$\begin{aligned} \hat{\psi}_{int}(\zeta, \eta) = & \frac{r_0 \sinh \zeta}{\sqrt{\cosh \zeta - \cos \eta}} \times \\ & \left\{ \sum_{n=0}^{M_{ia}} a_n^i P_{n-1/2}^1(\cosh \zeta) \cos(n\eta) + \sum_{n=1}^{M_{ib}} b_n^i P_{n-1/2}^1(\cosh \zeta) \sin(n\eta) \right\}. \end{aligned} \tag{5}$$

Functions $P_{n-1/2}^1$ and $Q_{n-1/2}^1$are the associated Legendre functions of the first and second kind, of degree one and half integer order [14], that are called toroidal harmonics when evaluated at $\cosh \zeta$. To carry out the decomposition, one must choose the basis functions degrees appropriately by defining integers $M_{ia}, M_{ib}, M_{ea}, M_{eb}$. Numerical stability of the final solution is highly dependent on this setting. Furthermore, complete decomposition is solved by determining a vector u of unknown decomposition coefficients in (4), (5), given by

$$\theta = (a_0^e, \ldots, a_{M_{ea}}^e, b_1^e, \ldots, b_{M_{eb}}^e, a_0^i, \ldots, a_{M_{ia}}^i, b_1^i, \ldots, b_{M_{ib}}^i). \tag{6}$$

This is done by minimizing cost function

$$J(\theta) = \sum_{i=1}^{N_f} \frac{(\hat{\psi}_i(\theta) - \tilde{\psi}_i^{meas})^2}{\sigma_f^2} + \sum_{i=1}^{N_s} \frac{(\delta_i \hat{\psi}(\theta) - \delta_i \tilde{\psi}^{meas})^2}{\sigma_s^2} + \sum_{i=1}^{N_B} \frac{(\hat{B}_i(\theta) - \tilde{B}_i^{meas})^2}{\sigma_B^2}. \tag{7}$$

Here, $\hat{B}$ is determined from$\hat{\psi}$ using

$$B = \frac{1}{r} \left(-\partial_z \psi, \partial_r \psi \right), \tag{8}$$

where σ_f^2, σ_s^2 and σ_B^2 are known variances of the measurement errors on the corresponding coils. Quantities $\tilde{\psi}_i^{meas}, \delta_i\tilde{\psi}^{meas}$ and $\tilde{B}_i^{meas}$ are computed from the measurements described above by subtracting the contribution of individual poloidal field coils. Vector θ can be utilized to reconstruct ψ in every point of coordinate system (r, z). Plasma boundary is identified as largest closed isoline of ψ (see Fig. 1).

Minimalization of (7) translates into equation

$$\mathrm{diag}(w)\tilde{y}(\tilde{\psi}^{meas}, \tilde{B}^{meas})^T = \mathrm{diag}(w)\tilde{A}(\hat{\psi}, \hat{B})\theta + e, \tag{9}$$

where $\tilde{y}(\tilde{\psi}^{meas}, \tilde{B}^{meas})^T \in \mathbb{R}^N, (N = N_f + N_s + N_B)$ are measurements extracted from individual coils,

$$w = (\underbrace{\sigma_f^{-1}, \cdots, \sigma_f^{-1}}_{N_f}, \underbrace{\sigma_s^{-1}, \cdots, \sigma_s^{-1}}_{N_s}, \underbrace{\sigma_B^{-1}, \cdots, \sigma_B^{-1}}_{N_B}) \tag{10}$$

is a vector of precisions of coils and diag(.) is a diagonal matrix with its argument on the main diagonal. Design matrix $\tilde{A}(\hat{\psi}, \hat{B}) \in \mathbb{R}^{N\times M}, (M = M_{ea} + M_{eb} + M_{ia} + M_{ib})$ comprises of evaluation of toroidal harmonics (4) and (5) in coordinates given by position of the measurement coils in chosen coordinate system, $e \in \mathbb{R}^N$ is the white noise with precision equal to β^{-1}. For further use, we rewrite equation (9) into a concise form

$$y = A\theta + e. \tag{11}$$

Because it was shown that precision of fit measured by MSE criterion does not translate directly into quality of final plasma boundary estimate, we shall use a different metric to assess it. We choose the *Hausdorff distance* with L_2 norm [15], which is for $O = \{o_1, ..., o_k\}$, $P = \{p_1, ..., p_l\}$, $o_i, p_i \in \mathbb{R}^m, \forall i$ defined as

$$D_H(O, P) = \max\left(\max_{o\ \in O}\min_{p\in P}\|o - p\|_2, \max_{p\in P}\min_{o\ \in O}\|o - p\|_2\right), \tag{12}$$

where $\|.\|_2$ is L_2 norm defined on $\mathbb{R}^m$. Further in the text, this metric is used to evaluate and compare output of the classical and regularized solution of the boundary reconstruction problem and a simulation.

It has been shown that the order of decomposition into toroidal harmonics significantly influences the quality of plasma boundary reconstruction. Furthermore, tested data showed that the best approach may not always be to estimate as many coefficients of the toroidal harmonics decomposition as possible. Also, the results of estimation are sensitive to the number of external and internal toroidal harmonics in a different way. We seek an optimal selection of the relevant elements of the model (11).

3. Bayesian Model Structure Identification

In this chapter, we will introduce theoretical principles of regularization, used to solve least square problem outlined in previous chapter. The conventional least squares formulation 11 corresponds to maximum likelihood estimation of likelihood function

$$p(y|A, \theta, \beta) = \mathcal{N}(y|A\theta, \beta^{-1}I). \tag{13}$$

where β is a precision parameter of the model error. The likelihood model alone cannot decide which structure of the model is relevant. This can be achieved by Bayesian treatment with carefully chosen prior distribution on unknown parameters [16].

3.1. Hierarchical prior - unknown prior variance

Hierarchical priors are a commonly used tool to achieve model structure selection. In this text, we use the automatic relevance determination mechanism [11] which is based on hierarchical prior of zero mean Gaussian with unknown variance. Specifically, we assume that the elements of vector θ are apriori independent with each vector having its own prior variance. Formally, we define

$$p(\theta|\alpha) = \mathcal{N}(0, \alpha^{-1}), \tag{14}$$
$$\alpha = \mathrm{diag}(\alpha_1, \alpha_2, \cdots, \alpha_M), \tag{15}$$
$$p(\alpha_i) = \mathcal{G}(a_0, b_0), \tag{16}$$
$$p(\beta) = \mathcal{G}(c_0, d_0), \tag{17}$$

where diag(.) is a diagonal matrix with elements of the argument vector on its diagonal.

Joint distribution of the likelihood (13) and the prior (14)–(16) is

$$p(y, \theta, \alpha, \beta|A) = p(y|A, \theta, \beta)p(\theta|\alpha)\prod_{i=1}^{M} p(\alpha_i)p(\beta). \tag{18}$$

The aim is to obtain posterior distribution of all unknown parameters, i.e. θ, α, β using the Bayes rule

$$p(\theta, \alpha, \beta|y, A) = \frac{p(y, \theta, \alpha, \beta|A)}{\int p(y, \theta, \alpha, \beta|A)d\theta d\alpha d\beta}. \tag{19}$$

Evaluation of the exact formula (19) is analytically intractable, therefore, we seek only aproximate marginals of the posterior distribution using Varitional Bayes. In further text, we drop A from all the conditional probabilities, as it is known and not a subject of estimation.

3.2. Variational Bayes Posterior

The Variational Bayes approximation is a specific form of the general divergence minimization framework [12]. It is based on the following theorem that provides conditions for analytical solution of a specific form of approximation.

Theorem 1. *Let $f(\theta|y)$ be the posterior distribution of multivariate parameter, $\theta = [\theta_1^T, \theta_2^T]^T$, and $\breve{p}(\theta|y)$ be an approximate distribution restricted to the set of conditionally independent distributions:*

$$\breve{p}(\theta|y) = \breve{p}(\theta_1, \theta_2|y) = \breve{p}(\theta_1|y)\,\breve{p}(\theta_2|y). \tag{20}$$

Any minimum of the Kullback-Leibler divergence from $\breve{p}(\cdot)$ to exact solution $p(\cdot)$

$$KL(\breve{p}(\theta|y)\,||p(\theta|y)) = \int \breve{p}(\theta|y) \ln \frac{\breve{p}(\theta|y)}{f(\theta|y)} d\theta, \tag{21}$$

is achieved when $\breve{p}(\cdot) = \tilde{p}(\cdot)$ where

$$\tilde{p}(\theta_i|y) \propto \exp\left(\mathsf{E}_{\tilde{p}(\theta_{/i}|y)}\{\ln(p(\theta, y))\}\right), \; i = 1, 2. \tag{22}$$

Here $\theta_{/i}$ denotes the complement of θ_i in θ. We will refer to $\tilde{p}(\theta_i|y)$ (22) as the VB-marginals. *Here, $\mathsf{E}_{f(\theta)}\{g(\theta)\}$ denotes expected value of function $g(\theta)$ with respect to distribution $p(\theta)$.*

Theorem 1 provides a powerful tool for approximation of joint pdfs in separable form [12]. A solution satisfying conditions (22) is typically found using an iterative algorithm.

The Variational Bayes method will be applied for the following conditional independence condition:

$$p(\theta, \alpha, \beta|y) = p(\theta|y)p(\alpha|y)p(\beta|y),$$

yileding conditions of optimality (22) in the form

$$p(\theta|y) \propto \exp\left(\mathsf{E}_{\tilde{p}(\alpha|y)\tilde{p}(\beta|y)}\left\{\ln\left(p\left(\theta, \alpha, \beta, y\right)\right)\right\}\right), \tag{23}$$

and equivalently for $\tilde{p}(\alpha|y)$ and $\tilde{p}(\beta|y)$. The functional forms of (23) are recognized to be of well known types

$$\begin{aligned}\tilde{p}(\alpha_i|y) &= \mathcal{G}(a_{\alpha i}, b_{\alpha i}),\\ \tilde{p}(\beta|y) &= \mathcal{G}(c, d),\\ \tilde{p}(\theta|y) &= \mathcal{N}(\hat{\theta}, S),\end{aligned}$$

with shaping parameters

$$a_{\alpha i} = a_{0i} + \frac{1}{2}, \qquad b_{\alpha i} = b_{0i} + \frac{1}{2}\widehat{\theta_i^2}. \tag{24}$$

$$c = c_0 + \frac{N}{2}, \qquad d = d_0 + \frac{1}{2}y^T y - y^T A\widehat{\theta} + \frac{1}{2}\widehat{\theta^T A^T A\theta} \tag{25}$$

$$\hat{\theta} = \widehat{\beta} S A^T y, \qquad S = (\widehat{\alpha} + \beta A^T A)^{-1} \tag{26}$$

The required moments of these distributions are:

$$\hat{\alpha}_i = \frac{a_{\alpha i}}{b_{\alpha i}}, \qquad \hat{\beta} = \frac{c}{d}$$

$$\widehat{\theta_i^2} = S_{ii} + \widehat{\theta_i}^2, \qquad \widehat{\theta\theta^T} = \hat{\theta}\hat{\theta}^T + S$$

The final estimation algorithm is described in Algorithm 1.

Algorithm 1 Iterative algorithm for structure selection of least squares model.

Off-line:

- select prior parameters a_{0i}, b_{0i}, c_0, d_0.
- select the number of iterations i_{max}, set iteration counter $i = 0$.

On-line:

- Initiate $p(\theta|y, x)$ by ordinary least squares solution: $\hat{\theta}^{(0)} = (A^T A)^{-1} A^T y$, $S^{(0)} = \frac{(y - A\hat{\theta}^{(0)})^T (y - A\hat{\theta}^{(0)})^T}{M - (N+1)} (A^T A)^{-1}$
- For i from 1 to i_{max}
  - update shaping parameters of α, using (24),
  - update shaping parameters of β, using (25),
  - update shaping parameters of θ,using (26),
- Report final estimate $\hat{\theta}^{(i_{max})}$ and compute plasma reconstruction

4. Experimental Validation

4.1. Tokamak COMPASS and data from a validated numerical model

Tokamak COMPASS is in operation in IPP CAS CR in Prague. On COMPASS, the process of plasma reconstruction through decomposition into a series of toroidal harmonics is implemented in VacTH code [17]. VacTH uses data measured on different types of magnetic coils to extrapolate plasma characteristics into the domain of the tokamak chamber [3].

In this paper, the performance of VacTH is evaluated on simulated data, for which the real shape of plasma boundary is known. These data are generated by the FREEBIE code [18] in inverse mode. To obtain such data, the geometry of the measuring coils and shape of the plasma boundary is chosen by the operator. Following that, appropriate feedback of every coil is computed and the corresponding set of magnetic measurements is generated. It is then used to recompute the plasma boundary via VacTH. The approach implemented in the VacTH to solve 11 is the ordinary least squares (OLS) without regularization. Among other characteristics, plasma boundary shape is obtained and can be directly compared with the original FREEBIE input (e.g. using Hausdorff distance 12).

For the purpose of this paper, all data were simulated with configuration of 16 magnetic coils and 4 saddle loops with parameters $\sigma_B = 10^{-3}, \sigma_f = \frac{10^{-1}}{2\pi}$, which agrees with the real configuration of the tokamak.

4.2. Results

Based on analysis of a training data set from the COMPASS tokamak, prior parameters of the VB approximation were determined as in table 1. This was done by substituting the OLS by LSARD (least squares automatic relevance determination) algorithm in VacTH, which produced different value of $\hat{\theta}$. With this new value, VacTH reconstructed a different shape of the plasma boundary. To asses performance of LSARD , Hausdorff distance between FREEBIE boundary and this reconstruction was computed. All boundaries were numerically interpolated into a large ($\sim 10^3$) number of points to assure more precise evaluation of similarity.

parameter	a_0	b_0	c_0	d_0	α_0	β_0
value	10^{-10}	10^{-10}	10^0	10^0	10^0	10^4

Table 1. Prior parameter settings for VB regularization.

Using prior parameters setting from table 1, performance of the LSARD algorithm was assessed on a test data set. On every tested equilibrium, plasma boundary was reconstructed using OLS, LSARD and RLS (regularized least squares) approximations. This was done for model of size$M = M_{ea} + M_{eb} + M_{ia} + M_{ib}$ (M is order of the toroidal harmonics decomposition), where $M \in \{5, ..., 22\}$ as the individual sums in (4) a (5) were extended with varying values of $M_{ea} \in \{0, ..., 6\}, M_{eb} \in \{1, ..., 6\}, M_{ia} \in \{0, ..., 4\}, M_{ib} \in \{1, ..., 4\}$. A comparison of methods is in Figure 4.2 for a number of different equilibria.

Because there are 20 measurements, we observe a clear deterioration of reconstruction with OLS as the problem of solving (11) becomes ill-conditioned for higher order M. On the other hand, reconstruction with LSARD or RLS is not affected by this fact. Although the performance of LSARD is worse in terms of the MSE statistic, plasma boundary reconstruction is more precise. This hints us that some sort of regularization is important for plasma boundary reconstruction problem, as some terms in the decomposition become obsolete with higher order of the problem. LSARD regularization clearly addresses this problem by iteratively minimizing the size of redundant terms of $\hat{\theta}$. Another important fact is that the quality of reconstruction using LSARD does not vary rapidly with changing value of M. This is important for actual implementation in VacTH code, as for computation in real time the exact choice of estimated

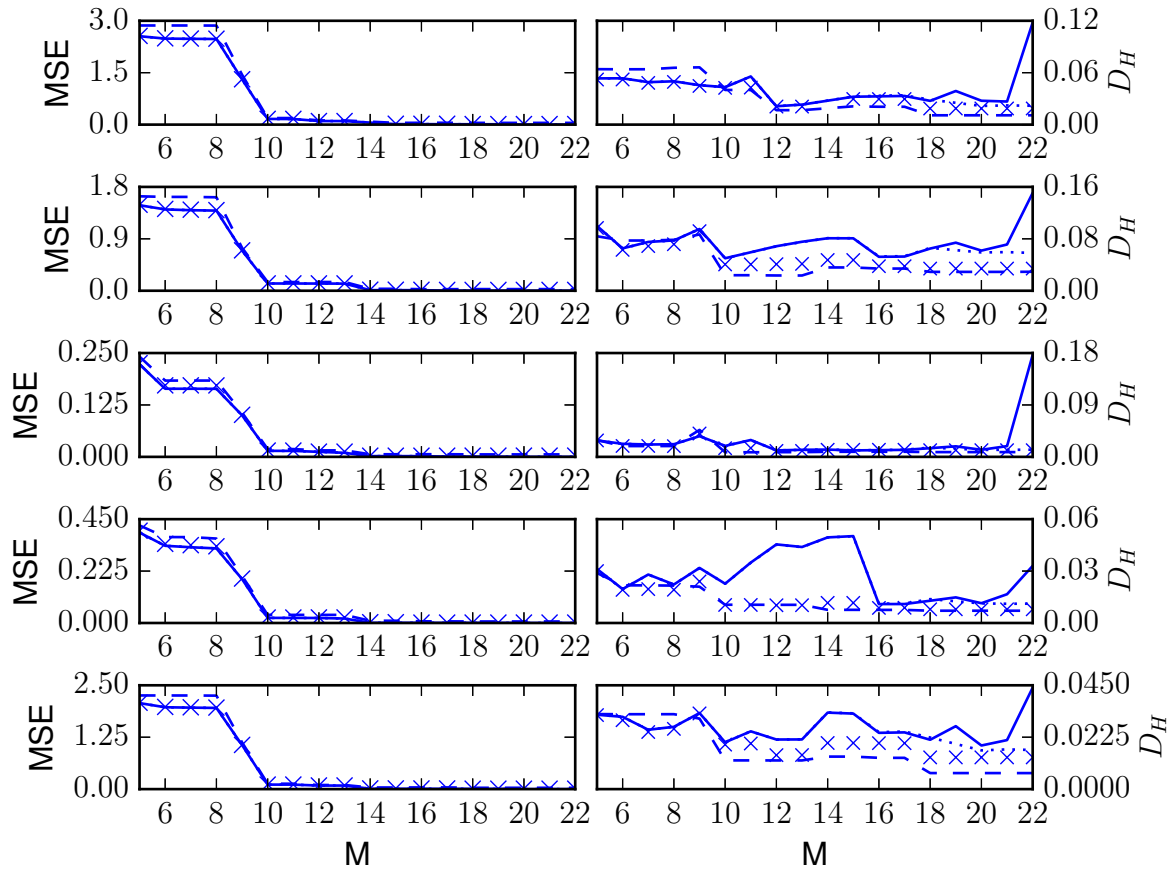

Figure 2. Results of plasma boundary reconstruction for varying order of toroidal harmonics decomposistion M for different plasma equilibria. Straight line is for OLS solution, dashed line for LSARD algorithm. Dotted line marks solution obtained with regularized least squares (RLS) with parameter $\lambda = 10$. Crossed line marks solution obtained with LASSO algorithm with parameter $\alpha = 1$. Besides MSE of fit, Hausdorff distance D_H between ground truth and solution obtained with respective solver is shown. Although the fit of LSARD method is worse than that of OLS, RLS or LASSO in terms of MSE, precision of boundary reconstruction is consistently better.

terms must be made in advance. Thus for LSARD we can simply choose M to be as large as possible to estimate with largest amount of information.

When analyzing more spherical shapes of plasma, prior parameter settings from 1 did not lead to significant improvement. It was shown that setting $a_0 = b_0 = 10^2$, which does not penalize large values of $\hat{\theta}$ as strictly, leads to improved results. These were still only slightly better than results obtained with OLS.

Finally, a comparison of plasma boundaries reconstructed using OLS, LSARD, LASSO regularization[19] and the original FREEBIE boundary is shown in Figure 3.

4.3. Offline model selection

Computational complexity of the current implementation of LSARD is too high and does not allow to replace OLS as the internal solver for real-time application in plasma reconstruction. Therefore, an attempt to determine an optimal model for which OLS is computed was made.

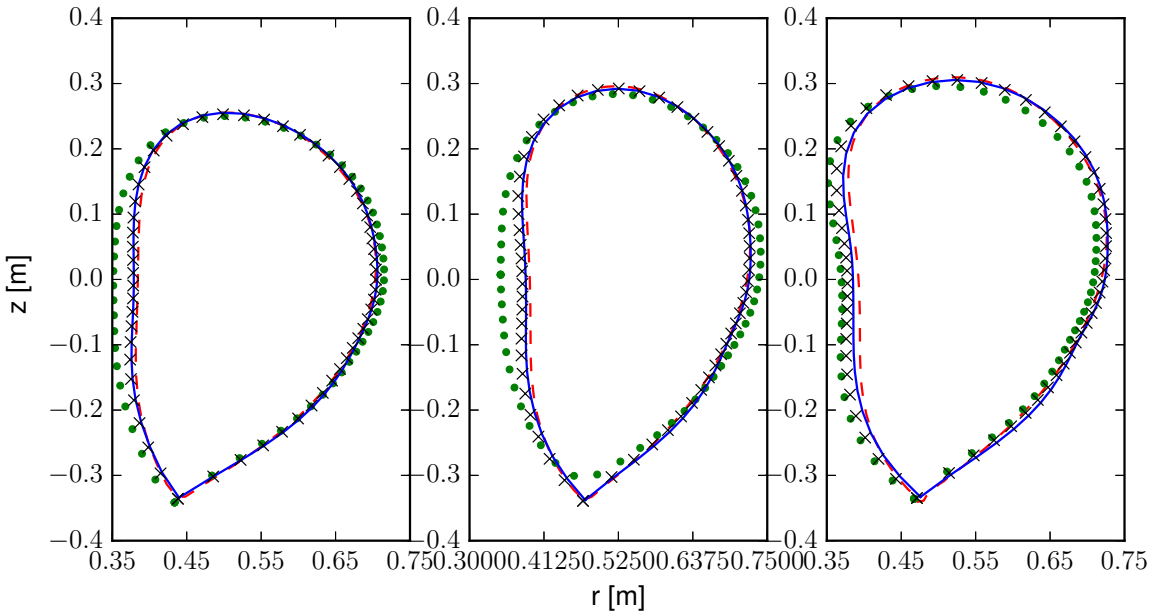

Figure 3. Comparison of plasma boundary reconstruction for three different equilibria for OLS implemented in VacTH (dotted line), LSARD (full line) and LASSO regularization with parameter $\alpha = 1$ (crossed line) using the same order of decomposition M. Ground truth, generated by FREEBIE algorithm, is denoted by dashed line.

Using sparsity property of ARD on a training data set, an optimal model was sequentially estimated by leaving out those terms of the model whose absolute value was smaller than a given constant $\delta \approx 10^{-4}$, until there were no more terms to omit in the estimation. Through this effort, a set of indices for sums (4) and (5) was obtained. This set is in Table 2. It holds that $n \in e_a$for the first sum in (4) etc. The ARD selected model is indeed very sparse when compared with the full model.

The three models were validated against each other on a distinct set of equilibria. OLS implemented in VacTH were used to compute $\hat{\theta}$ for each respective model structure. Then, plasma boundary was reconstructed. Graphical evaluation is in Figure 4. No distinct improvement from the full model to ARD selected model can be observed, although the results of ARD selected model are much more consistent.

	full model	model selected using ARD	control model
e_a	$(0, 1, 2, 3, 4, 5)$	-	$(0,\ 1,\ 2)$
e_b	$(1, 2, 3, 4, 5)$	-	$(1,\ 2)$
i_a	$(0, 1, 2, 3)$	$(0,\ 1,\ 2)$	$(0,\ 1,\ 2,\ 3)$
i_b	$(1, 2, 3)$	(1)	$(1,\ 2,\ 3)$

Table 2. Sets of indices, determining structure of estimated model.

5. Conclusion

The presented method of model selection has been shown to provide consistently better results on the problem of plasma boundary estimation compared to the conventional approach. It has been shown that a model with fewer carefully selected parameters avoids the overfitting problem

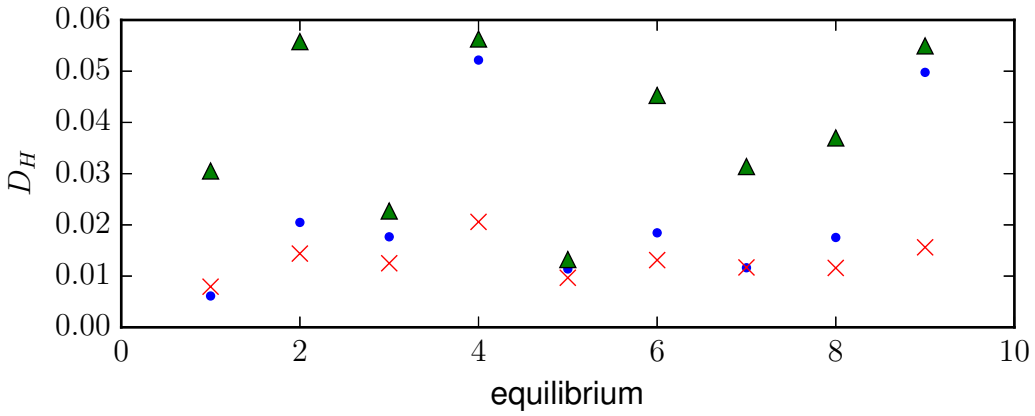

Figure 4. Comparison of full model (denoted by dots), control model (triangles) and model selected via the ARD principle (crosses) performance on different equilibria. D_H is the Hausdorff distance between the original FREEBIE boundary and the reconstruction. Notably more consistent performance of the sparse model structure selected by the ARD principle can be observed in comparison to full and control model as defined in 2.

and thus achieves better reconstruction of the overall shape of the plasma boundary. This has been achieved on simulated data from a detailed model. The complexity of the computation is intentionally kept low so that the algorithm can be run in real time on existing hardware.

References

[1] Ambrosino G and Albanese R 2005 *IEEE Control Systems Magazine* **25** 76–92
[2] Ariola M and Pironti A 2008 *Magnetic control of tokamak plasmas* (Springer Science & Business Media)
[3] Faugeras B, Blum J, Boulbe C, Moreau P and Nardon E 2014 *Plasma Physics and Controlled Fusion* **56** 114010
[4] Scott J G, Berger J O *et al.* 2010 *The Annals of Statistics* **38** 2587–2619
[5] O'Hara R B, Sillanpää M J *et al.* 2009 *Bayesian analysis* **4** 85–117
[6] George E I and McCulloch R E 1993 *Journal of the American Statistical Association* **88** 881–889
[7] Ruggieri E and Lawrence C E 2012 *Computational Statistics & Data Analysis* **56** 1319 – 1332 ISSN 0167-9473
[8] Ghosh J and Tan A 2015 *Computational Statistics & Data Analysis* **81** 76 – 88 ISSN 0167-9473
[9] Carbonetto P, Stephens M *et al.* 2012 *Bayesian Analysis* **7** 73–108
[10] Zhao K and Lian H 2014 *Computational Statistics & Data Analysis* **80** 223 – 239 ISSN 0167-9473
[11] Tipping M 2001 *The journal of machine learning research* **1** 211–244
[12] Šmídl V and Quinn A 2005 *The Variational Bayes Method in Signal Processing* (Springer)
[13] Šmídl V and Quinn A 2008 *IEEE Transactions on Signal Processing* **56** 5020–5030
[14] Lebedev N N and Silverman R A 1972 *Special functions and their applications* (Courier Corporation)
[15] Huttenlocher D P, Klanderman G, Rucklidge W J *et al.* 1993 *Pattern Analysis and Machine Intelligence, IEEE Transactions on* **15** 850–863
[16] Bishop C 2006 *Pattern recognition and machine learning* vol 1 (springer New York)
[17] Urban J, Appel L C, Artaud J F, Faugeras B, Havlicek J, Komm M, Lupelli I and Peterka M 2015 *Fusion Engineering and Design* **96-67** 998–1001
[18] Artaud J and Kim S 2012 *EPS Conference on Plasma Physics*
[19] Tibshirani R 1996 *Journal of the Royal Statistical Society. Series B (Methodological)* 267–288